

# Measurement of the Transverse Beam Spin Asymmetry in Elastic Electron Proton Scattering and the Inelastic Contribution to the Imaginary Part of the Two-Photon Exchange Amplitude

F. E. Maas,<sup>1,\*</sup> K. Aulenbacher,<sup>1</sup> S. Baunack,<sup>1</sup> L. Capozza,<sup>1</sup> J. Diefenbach,<sup>1</sup> B. Gläser,<sup>1</sup> Y. Imai,<sup>1</sup> T. Hammel,<sup>1</sup> D. von Harrach,<sup>1</sup> E.-M. Kabuß,<sup>1</sup> R. Kothe,<sup>1</sup> J. H. Lee,<sup>1</sup> A. Sanchez-Lorente,<sup>1</sup> E. Schilling,<sup>1</sup> D. Schwaab,<sup>1</sup> G. Stephan,<sup>1</sup> G. Weber,<sup>1</sup> C. Weinrich,<sup>1</sup> I. Altarev,<sup>2</sup> J. Arvieux,<sup>3</sup> M. Elyakoubi,<sup>3</sup> R. Frascaria,<sup>3</sup> R. Kunne,<sup>3</sup> M. Morlet,<sup>3</sup> S. Ong,<sup>3</sup> J. Vandewiele,<sup>3</sup> S. Kowalski,<sup>4</sup> R. Suleiman,<sup>4</sup> and S. Taylor<sup>4</sup>

<sup>1</sup>*Institut für Kernphysik, Johannes Gutenberg-Universität Mainz, J.-J.-Becherweg 45, D-55099 Mainz, Germany*

<sup>2</sup>*St. Petersburg Institute of Nuclear Physics, Gatchina, Russia*

<sup>3</sup>*Institut de Physique Nucleaire, 91406 - Orsay Cedex, France*

<sup>4</sup>*Laboratory for Nuclear Science, Massachusetts Institute of Technology, Cambridge, MA 02139, USA*

(Dated: June 23, 2018)

We report on a measurement of the asymmetry in the scattering of transversely polarized electrons off unpolarized protons,  $A_{\perp}$ , at two  $Q^2$  values of  $0.106 \text{ (GeV/c)}^2$  and  $0.230 \text{ (GeV/c)}^2$  and a scattering angle of  $30^\circ < \theta_e < 40^\circ$ . The measured transverse asymmetries are  $A_{\perp}(Q^2 = 0.106 \text{ (GeV/c)}^2) = (-8.59 \pm 0.89_{\text{stat}} \pm 0.75_{\text{sys}}) \times 10^{-6}$  and  $A_{\perp}(Q^2 = 0.230 \text{ (GeV/c)}^2) = (-8.52 \pm 2.31_{\text{stat}} \pm 0.87_{\text{sys}}) \times 10^{-6}$ . The first errors denotes the statistical error and the second the systematic uncertainties.  $A_{\perp}$  arises from the imaginary part of the two-photon exchange amplitude and is zero in the one-photon exchange approximation. From comparison with theoretical estimates of  $A_{\perp}$  we conclude that  $\pi$ N-intermediate states give a substantial contribution to the imaginary part of the two-photon amplitude. The contribution from the ground state proton to the imaginary part of the two-photon exchange can be neglected. There is no obvious reason why this should be different for the real part of the two-photon amplitude, which enters into the radiative corrections for the Rosenbluth separation measurements of the electric form factor of the proton.

PACS numbers: 11.30.Er, 13.40.-f, 13.40.Gp, 13.60.Fz, 13.88.+e, 14.20.Dh, 23.40.Bw, 24.70.+s, 24.85.+p, 25.30.Bf, 25.30.Rw

The simple interpretation of electromagnetic probe experiments like elastic scattering of electrons off protons is due to the smallness of the electromagnetic coupling constant  $\alpha \approx 1/137$  which allows to approximate the electromagnetic transition amplitude as a single photon exchange process (Born approximation). Higher order processes are treated as small “radiative corrections” like the two-photon exchange which is schematically shown in Fig. 1. It involves the exchange of two virtual photons

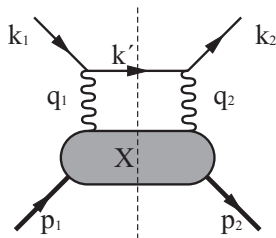


FIG. 1: The two-photon exchange diagram. The filled blob X represents the response of the nucleon to the scattering of the virtual photon.

tons (bosons) and an intermediate hadronic state which includes the ground-state and all excited states of the hadronic system, which can be off-shell for the real part of this box diagram amplitude. This makes the theoretical computation of the two-photon effects difficult. Tests of the limits of the validity of the one-photon ap-

proximation have been done in the past, using different methods, like comparison of the  $e^+p$  and  $e^-p$  cross section data,  $\epsilon$ -linearity of the ratio  $R^2 = (\mu_p G_E^p / G_M^p)^2$  in the Rosenbluth formula or observation of T-odd polarization observables [1]. No effect has been found within the accuracy of the experiments. This discussion has been reactivated recently by the observation that the ratio of the electric form factor of the proton to the magnetic form factor,  $R = (\mu_p G_E^p / G_M^p)$ , is different when measured by the method of Rosenbluth separation as compared to the extraction from polarization transfer. The determination of the ratio  $R$  from longitudinal-transverse (LT) or Rosenbluth separation yields a value for  $R$  which is consistent with  $R \approx 1$  [2, 3, 4, 5] in a  $Q^2$  range  $< 6 \text{ (GeV/c)}^2$ . Recent polarization transfer measurements at Jefferson Laboratory [6, 7] measure  $R$  from the ratio of the transverse to longitudinal polarizations of the recoil proton, yielding a very different result  $R \approx 1 - 0.135(x - 0.24)$  where  $x = Q^2$  in units of  $(\text{GeV/c})^2$ . It has been suggested [8, 9] that a contribution from two-photon exchange can explain such a discrepancy. There are observables which are directly sensitive to two-photon effects, like the transverse asymmetry  $A_{\perp}$  in the elastic scattering of transversely polarized electrons off unpolarized nucleons.  $A_{\perp}$  arises from the interference of the one-photon with the two-photon exchange amplitude and is zero in Born approximation.

The treatment of the exchange of many photons is done in a framework similar to the one developed for elastic  $np$ -scattering [10]. The parametrization of the scattering-amplitude consists of a set of six complex functions, e.g.  $\hat{G}_M(s, Q^2)$ ,  $\hat{G}_E(s, Q^2)$ , and  $\hat{F}_i(s, Q^2)$ ,  $i = 3..6$ , which are generalized form factors. The evaluation of the elastic cross section  $d\sigma/d\Omega$  for the scattering of electrons off protons has been discussed as well as quantities like the polarization transfer from the electron to the nucleon,  $P_l$  and  $P_t$ , the electron-positron beam charge asymmetry, the target recoil normal spin asymmetry, the transverse beam spin asymmetry ( $A_\perp$ ), the depolarization tensor and other variables [11, 12, 13, 14, 15]. For example the differential cross section for elastic electron-nucleon scattering can be expressed as:

$$\frac{d\sigma}{d\Omega} = \sigma_0 \left\{ |\hat{G}_M|^2 + \frac{\epsilon}{\tau} |\hat{G}_E|^2 + 2\epsilon \sqrt{\tau(1+\tau)} \frac{1+\epsilon}{1-\epsilon} \left[ \frac{1}{\tau} |\hat{G}_E| + |\hat{G}_M| \right] \mathcal{R}(\hat{F}_3(s, Q^2)) + \mathcal{O}(e^4) \right\} \quad (1)$$

The two-photon contribution appears in the real part of the amplitude  $\mathcal{R}(\hat{F}_3(s, Q^2))$ . An ab initio calculation of the real part of  $\hat{F}_3(s, Q^2)$  is at present impossible. It would require the knowledge of the off-shell form factors of the proton in the intermediate state and all possible excitation amplitudes for the intermediate state and their off-shell transition form factors. A recent model calculation gives a contribution to the cross section on the order of a few percent [16]. The authors used the ad hoc assumptions that the intermediate state is described by an on-shell particle and by the ground state only. A parton model calculation which is applicable at the high  $Q^2$  employed for the Rosenbluth data [17] yields a quantitative agreement with the polarization transfer measurements. As only the imaginary part of the two-photon amplitude contributes via the interference with the one-photon exchange amplitude [1] to  $A_\perp$ ,  $A_\perp$  is proportional to the imaginary part of the combination of  $\hat{F}_3(s, Q^2)$ ,  $\hat{F}_4(s, Q^2)$ , and  $\hat{F}_5(s, Q^2)$ . The evaluation of  $A_\perp$  yields [11, 18]:

$$A_\perp = \frac{m_e}{M} \sqrt{2\epsilon(1-\epsilon)} \frac{\sqrt{1+\tau}}{\tau} \left(1 + \frac{\epsilon}{\tau} \frac{G_E^2}{G_M^2}\right)^{-1} \times \left(-\tau \mathcal{I}\left(\frac{\hat{F}_3}{G_M}\right) - \frac{G_E}{G_M} \mathcal{I}\left(\frac{\hat{F}_4}{G_M}\right) - \frac{1}{1+\tau} \left(\tau + \frac{G_E}{G_M}\right) \mathcal{I}\left(\frac{\nu \hat{F}_5}{M^2 G_M}\right)\right) + \mathcal{O}(e^4). \quad (2)$$

$\mathcal{I}(\hat{F}_i(s, Q^2))$  denotes the imaginary part of  $\hat{F}_i(s, Q^2)$  and  $\nu$  is the energy transfer to the proton. The order of magnitude of  $A_\perp$  is given by the factor  $m_e/M \approx 5 \times 10^{-4}$ . At present, there is little information from experiments concerning  $\hat{F}_3(s, Q^2)$ ,  $\hat{F}_4(s, Q^2)$ , and  $\hat{F}_5(s, Q^2)$ .

In contrast to the real part of the two-photon exchange contribution, the imaginary part of the two-photon amplitude can be calculated from the absorptive part of

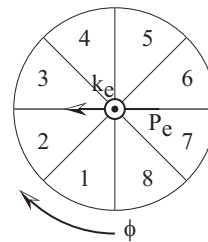


FIG. 2: The momentum vector  $\vec{k}_e$  is pointing here out of the paper plane. The momentum vector  $\vec{k}_{out}$  of the outgoing electron can take all possible  $\phi_e$  values. Both together define the coordinate system according to the Madison convention [20] with  $\vec{S}_n = (\vec{k}_e \times \vec{k}_{out})/|\vec{k}_e \times \vec{k}_{out}|$ . The direction of the electron polarization vector  $\vec{P}_e$  for the + helicity state is indicated by the arrow.  $\phi_e$  and  $\phi_{\vec{P}_e}$  are counted as indicated. The elastic scattered electrons are detected in the  $\phi_e$ -symmetric PbF<sub>2</sub>-calorimeter of the A4 experiment. For the extraction of  $A_\perp^m$ , the detector has been divided into 8 sectors as indicated in the figure.

the doubly virtual Compton scattering tensor with two space-like photons [11]. The momenta of the boson and fermion in the loop are given by momentum conservation. All intermediate hadronic states, which can be excited due to the kinematics, contribute to  $A_\perp$ . The calculation of  $A_\perp$  on the proton at low  $Q^2$  requires known quantities, like elastic scattering form factors of the proton (elastic contribution) and transition amplitudes to  $\pi N$ -intermediate states (inelastic contribution). The SAMPLE collaboration has recently reported on the first measurement of  $A_\perp$  at a laboratory scattering angle of  $130^\circ < \theta_e < 170^\circ$  and a  $Q^2$  of 0.1 (Gev/c)<sup>2</sup> [19]. We report here on a measurement of  $A_\perp$  at similar  $Q^2$ , but much higher energy, and at forward angle. Thus, we are not only sensitive to the ground state as in the case of the SAMPLE measurements, but also to  $\pi N$ -intermediate states. In addition, both photons are space like in forward scattering while in contrast at backward angles the asymmetry is dominated by cases where one of the photons is quasi real [11].  $A_\perp$  is an asymmetry in the cross section for the elastic scattering of electrons with spin parallel ( $\sigma_\uparrow$ ) and spin anti-parallel ( $\sigma_\downarrow$ ) to the normal scattering vector defined by  $\vec{S}_n = (\vec{k}_e \times \vec{k}_{out})/|\vec{k}_e \times \vec{k}_{out}|$ .  $\vec{k}_e$  and  $\vec{k}_{out}$  are the three-momentum vectors of the initial and final electron state. The measured asymmetry  $A_\perp^m$  can be written as  $A_\perp^m = (\sigma_\uparrow - \sigma_\downarrow)/(\sigma_\uparrow + \sigma_\downarrow) = A_\perp \vec{P}_e \cdot \vec{S}_n$ .  $A_\perp$  is a function of the scattering angle  $\theta_e$ , the four-momentum transfer  $Q^2$  and the electron beam energy  $E_e$ . The term  $\vec{P}_e \cdot \vec{S}_n$  introduces a dependence of  $A_\perp^m$  on the electron azimuthal scattering angle  $\phi_e$  with a zero crossing for the case where the scattering plane contains the incident electron polarization vector  $\vec{P}_e$ .  $A_\perp^m$  vanishes for  $\theta_e = 0^\circ$  (forward scattering) and for  $\theta_e = 180^\circ$  (backward scattering). It vanishes also if the electron polarization vector is longitudinal. Fig. 2 shows a schematic defining

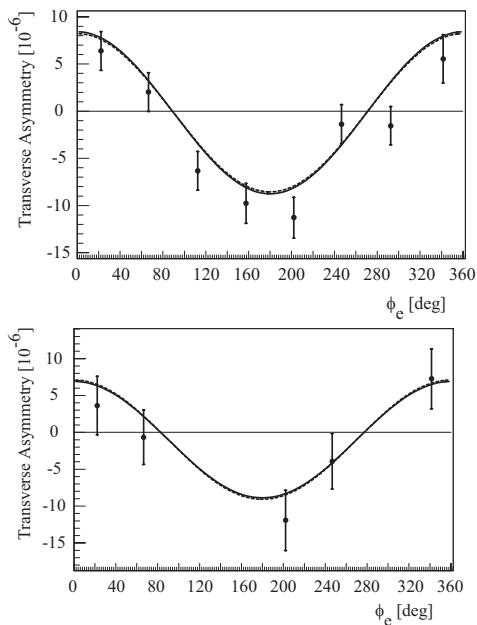


FIG. 3: The upper plot shows the result of our measurements of  $A_{\perp}$  for a beam energy of 569.31 MeV and at the lower plot for the beam energy of 855.15 MeV. The asymmetry is plotted as a function of the laboratory angle  $\phi_e$  as defined in Fig. 2. The 1022 PbF<sub>2</sub>-detectors of the calorimeter have been divided into 8 subsets (sector 1 to 8), each spanning an angular range of  $\approx 45^\circ$  in  $\phi_e$ . For the lower plot only 756 channels of the PbF<sub>2</sub>-detector had been installed (sector 1, 2, 5, 6, and part of sector 8).

$\phi_e$ ,  $\vec{S}_n$ , and other quantities.

We have used the apparatus of the A4 experiment at the MAMI accelerator in Mainz to make a measurement of the transverse beam spin asymmetry  $A_{\perp}$  [21, 22, 23, 24]. The polarized electrons were produced using a strained layer GaAs crystal which is illuminated with circularly polarized laser light [25] resulting in longitudinally polarized electrons. The sign of the electron beam polarization was switched between the two patterns  $(+ - - +)$  and  $(- + + -)$  randomly by means of a fast Pockels cell in the optical system of the polarized electron source. Average beam polarization was about 80% which has been measured using a Møller polarimeter in a different experimental hall. The longitudinal spin of the electrons leaving the photocathode has been rotated in the accelerator plane using a Wien filter located between the 100 keV polarized electron source and the injector linac of the accelerator. In addition the energy of the accelerator has been tuned so that the relativistic spin precession in the three microtron stages of the accelerator in combination with the Wien filter resulted in a beam polarization perpendicular to the beam direction. The rotation of the spin angle at the location of the experiment has been measured using the transmission Compton polarimeter located between the liquid hydrogen target and the elec-

tron beam dump.

The measurements of  $A_{\perp}^m$  have been done with the Wien filter set so that the electron polarization vector  $\vec{P}_e$  shows for the + helicity to the negative x-axis of a right handed coordinate system according to the Madison convention [20] and as indicated in Fig. 2, corresponding to  $\phi_{\vec{P}_e} = 90^\circ$  and  $\theta_{\vec{P}_e} = 90^\circ$ . In this case the sign of  $A_{\perp}^m$  as measured in sectors 4 and 5 (corresponding to  $\phi_{\vec{P}_e} = 180^\circ$ ) is the same as  $A_{\perp}$  and the sign of  $A_{\perp}^m$  as measured in sectors 1 and 8 is opposite to  $A_{\perp}$ . The transmission Compton polarimeter allowed to set the angle of the beam polarization vector to an accuracy of  $\delta\theta_{\vec{P}_e} = \pm 1.6^\circ$  and  $\delta\phi_{\vec{P}_e} = \pm 0.9^\circ$  for the beam energy of 855.15 MeV and 569.31 MeV, respectively. For the measurements of  $A_{\perp}$  a polarized electron beam of 20  $\mu\text{A}$  has been scattered off a 10 cm liquid hydrogen target. The scattered particles have been detected under a scattering angle of  $30^\circ < \theta_e < 40^\circ$  in the PbF<sub>2</sub>-calorimeter, which has a solid angle of 0.62 sr and measures the energy of the scattered particles deposited in the 1022 PbF<sub>2</sub> crystals. The detector is  $\phi_e$ -symmetric around the beam axis. The luminosity is permanently measured by 8 water-Cerenkov detectors located at small electron scattering angles  $4^\circ < \theta_e < 10^\circ$ , symmetric around  $\phi_e$ . The luminosity monitors have been optimized for the detection of Møller scattering. The transverse beam spin asymmetry in Møller scattering is of the same order as in elastic electron proton scattering [26]. Using the  $\phi_e$ -symmetry of the luminosity detectors we average over the 8 luminosity monitors before normalizing target density fluctuations to the luminosity signal in the extraction of the asymmetry.

We have measured  $A_{\perp}^m$  at two different beam energies of 569.31 MeV and at 855.15 MeV corresponding to an acceptance averaged four-momentum transfer of 0.106 (GeV/c)<sup>2</sup> and 0.230 (GeV/c)<sup>2</sup>, respectively. The same method of inserting a  $\lambda/2$ -plate in the laser system of the source as described in [24] has been applied in order to minimize false asymmetries and test for systematic errors. The transverse beam spin asymmetry and the associated systematic error has been determined using the same analysis method after correcting for beam polarization, target density fluctuations, nonlinearities in the luminosity monitors and dead time in the calorimeter as in [24]. The  $\phi_e$  dependence of the measured  $A_{\perp}^m$  leads to a complete cancelation of the transverse asymmetry if averaged over the  $\phi_e$ -symmetric detector. Therefore we have made 8 subsets of the 1022 detector channels of the PbF<sub>2</sub>-calorimeter, each subset spanning a sector of  $45^\circ$  in  $\phi_e$ . The result of our measurements can be seen in Fig. 3. The data at 569.31 MeV and at 855.15 MeV represent 54 h and 46 h of data taking time, respectively. One sees a clear  $\cos(\phi_e)$ -modulation as expected from  $A_{\perp}^m$  taking into account our definition of  $\phi_e$  in Fig. 2. The solid lines in Fig. 3 represent a fit to the data

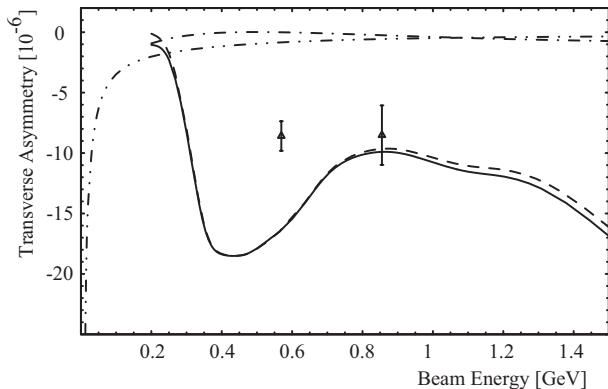


FIG. 4: The results of two model calculations [11, 27] are shown with the results of our measurements of  $A_{\perp}$  (see text for explanation).

points of the form  $A_{\perp}^m = A_{\perp} \int_{(\phi_e - 22.5^\circ)}^{(\phi_e + 22.5^\circ)} \cos(\phi'_e) d\phi'_e = 0.765 A_{\perp} \cos(\phi_e)$ . Including all corrections, we obtain a value of  $A_{\perp}(Q^2 = 0.106(\text{GeV}/c)^2) = (-8.59 \pm 0.89_{\text{stat}} \pm 0.75_{\text{sys}})$  ppm and  $A_{\perp}(Q^2 = 0.230(\text{GeV}/c)^2) = (-8.52 \pm 2.31_{\text{stat}} \pm 0.87_{\text{sys}})$  ppm. The first error represents in both cases the statistical error and the second the systematic uncertainties. In Fig. 4 our measured asymmetries are compared to calculations from [11]. For the intermediate hadronic state the ground state proton (elastic contribution, dash-dotted line) has been used together with excitation amplitudes to  $\pi\text{N}$ -intermediate states (inelastic contribution, dashed line) as described by MAID [28]. The solid line shows the result for the full calculation. The dash-double-dotted line represents the results from a calculation using an effective theory of electrons, protons and photons [27] which should be compared to the elastic contribution. The data points are the results of our measurement at 569.31 MeV and at 855.15 MeV. Our measurements of  $A_{\perp}$  clearly show that the two-photon exchange contribution is already dominated at our low- $Q^2$ -kinematics of  $Q^2=0.106 \text{ GeV}^2$  and  $Q^2=0.230 \text{ GeV}^2$  to a large extent by the inelastic  $\pi\text{N}$ -intermediate state of  $\Delta(1232)$ -resonance and higher resonances.

The extraction of  $\mathcal{I}(\hat{F}_3(s, Q^2))$ ,  $\mathcal{I}(\hat{F}_4(s, Q^2))$ , and  $\mathcal{I}(\hat{F}_5(s, Q^2))$  from a measurement of  $A_{\perp}$  is in principle possible. The knowledge of the imaginary part of  $\hat{F}_3(s, Q^2)$  can be used to calculate the real part of  $\hat{F}_3(s, Q^2)$ , for example by applying dispersion relations. This would give the unique possibility of comparing a model calculation for the real part of  $\hat{F}_3(s, Q^2)$  with the extraction done from the measurement of the imaginary part. Such an experimental verification of the two-photon contribution to the cross section is at present impossible due to the lack of data. We plan on a series of measurements of  $A_{\perp}$  at different beam energies under forward and backward angles [29]. Testing the theoretical framework used to compute them is important for the interpretation of measurements testing the

Standard Model. In particular this applies to the neutron  $\beta$ -decay correlation experiments. Combined with the neutron lifetime they allow a determination of the Kobayashi-Maskawa matrix element  $V_{ud}$  that is free from nuclear theory uncertainties. Similarly, the Q-weak experiment at Jefferson Lab will test the Standard Model running of  $\sin^2 \theta_W$ . Any discrepancies between the Standard Model predictions for these quantities and the experimental values could point to physics beyond the Standard Model, to the extent that theoretical uncertainties in the Standard Model radiative corrections can be shown to be sufficiently small. In addition to the implications for the electroweak physics and physics beyond the Standard Model, this opens the possibility to access the doubly virtual Compton scattering tensor of the neutron by measuring  $A_{\perp}$  on the deuteron.

This work is supported by the Deutsche Forschungsgemeinschaft in the framework of the SFB 201, SPP 1034, by the IN2P3 of CNRS and in part by the US Department of Energy. We are indebted to K.H. Kaiser and the whole MAMI crew for their tireless effort to provide us with good electron beam. We also would like to thank the A1 Collaboration for the use of the Møller polarimeter. We would like to thank M. Gorshteyn, B. Pasquini, M. Ramsey-Musolf and M. Vanderhaeghen for useful discussions.

---

\* corresponding author: maas@kph.uni-mainz.de

- [1] A. D. Rujula et al., Nucl. Phys. B **35**, 365 (1971).
- [2] R. G. Arnold et al., Phys. Rev. Lett. **35**, 776 (1975).
- [3] R. C. Walker et al., Phys. Rev. D **49**, 5671 (1994).
- [4] L. Andivahis et al., Phys. Rev. D **50**, 5491 (1994).
- [5] J. Arrington, Phys. Rev. D **69**, 032201 (2003).
- [6] M. K. Jones et al., Phys. Rev. Lett. **84**, 1398 (2000).
- [7] O. Gayou et al., Phys. Rev. Lett. **88**, 092301 (2002).
- [8] P. Guichon et al., Phys. Rev. Lett. **91**, 142303 (2003).
- [9] S. J. Brodsky et al., Phys. Rev. D **69**, 054022 (2004).
- [10] M. L. Goldberger et al., Ann. of Phys. **2**, 226 (1957).
- [11] B. Pasquini et al., hep-ph/0405303 (2004).
- [12] M. P. Rekalov et al., nucl-th/0307066 (2003).
- [13] M. P. Rekalov et al., nucl-th/0402004 (2004).
- [14] S. D. Drell and J. D. Sullivan, Phys. Lett. **19**, 516 (1965).
- [15] M. P. Rekalov et al., Nucl. Phys. A **740**, 271 (2004).
- [16] P. G. Blunden et al., Phys. Rev. Lett. **91**, 142304 (2003).
- [17] Y. C. Chen et al., Phys. Rev. Lett. **93**, 122301 (2004).
- [18] M. Gorchtein et al., Nucl. Phys. A **741**, 234 (2004).
- [19] S. Wells et al., Phys. Rev. C **63**, 064001 (2001).
- [20] H. H. Barschall and W. Haeberli, eds., *Polarization phenomena in nuclear reactions* (The University of Wisconsin Press, 1970).
- [21] H. Euteneuer et al., Proc of the EPAC 1994 **1**, 506 (1994).
- [22] F. E. Maas et al., *Proc. of the ICATPP-7* (World Scientific, 2002), chap. Crystal Detectors, p. 758.
- [23] F. E. Maas et al., Eur. Phys. J. A **17**, 339 (2003).
- [24] F. E. Maas et al., Phys. Rev. Lett. **93**, 022002 (2004).
- [25] K. Aulenbacher et al., Nucl. Ins. Meth. A **391**, 498 (1997).
- [26] L. Dixon et al., Phys. Rev. D **69**, 113001 (2004).

- [27] L. Diaconescu et al., nucl-th/0405044 (2004). (2004).
- [28] D. Drechsel et al., Nucl. Phys. **A 645**, 145 (1999).
- [29] DFG proposal SFB 443:H7, Spokesperson: F. E. Maas